XLI CILAMCE
XLI Ibero-Latin American Congress on Computational Methods in Engineering
16-19 November, 2020 FOZ DO IGUAÇU PARANÁ - BRAZIL

Determination of the heat treatment curve for machine components of power generation plants using finite element analysis

Esteban Foronda[1], Miguel Villa[1], Sebastián Cure[1], Wilfredo Montealegre Rubio[1]

[1]*Departamento de Ingeniería Mecánica, Universidad Nacional de Colombia*
Cra. 65 #59a-110, 050034, Medellín, Colombia
eforondao@unal.edu.co, mavillag@unal.edu.co, scurez@unal.edu.co, wmontealegrer@unal.edu.co

Abstract. Heat treatment cycles allow stress relieving of machine components of hydroelectric and thermoelectric plants. Differences between the heating/cooling rate of surface and core of these components during the three heat treatment stages (heating, holding and cooling) lead to thermal deformation and stresses that need to be controlled to avoid failure. Finite element analysis is used in this work to determine the optimal heating/cooling rate to guarantee that the components subjected to heat treatment in a radiant tubes furnace do not suffer damage at any stage of the process. The results of this work are focused on a Francis turbine runner, which is a critical component in this industry due to its size, geometrical complexity and maintenance costs. Transient thermo-structural analysis is implemented in commercial software with non-linear properties. In addition, the proposed numerical approach allows evaluating the maximum power requirement of the furnace to follow the heat treatment curve. The results indicate that the lower the heating/cooling rate, the greater the thermal uniformity obtained within the turbine runner; therefore, there is less risk of mechanical damage. However, the final decision on the heat treatment rate depends on the duration constraints of the process.

Keywords: FEA, heat treatment, thermal transient analysis, Furnace.

1 Introduction

Hydroelectric and thermoelectric machine components are subjected to heat treatment during maintenance and repair activities, following three stages: heating, holding and cooling. The time it takes for the components to reach the holding (ambient) temperature from ambient (holding) temperature determines the heating (cooling) rate of the process. Transient thermal gradients create differences between the heating and cooling rates of the surface and the core of the components, generating thermal deformations and stresses.[1]

Li et al. [3] and Hao et al. [4] conducted a comparison between numerical and experimental analysis of the heat treatment of components subjected to 950°C in a vacuum furnace with automatic temperature control. Their works were focused on reaching a homogenous temperature by optimizing the heat treatment parameters. They concluded that thermal uniformity is reached for parts with thickness lower than 50mm if the maximum difference between the temperature of the center and the external surface is kept below 50°C. This allows eliminating internal distortions and damage of the components during the heat treatment. These results were supported for heating rates of 6 and 12 °C/min. Wan, Dong, Li y Liu [5] designed a non-linear transient simulation for the heat treatment of a 22cm thick plate up to 1280°C, assessing the effect of the temperature and the heating rate on thermal stresses. Due to the high temperature of the plate, radiation was the main heat transfer mechanism and convection was considered by using a combined heat transfer coefficient. These authors and Ramanenka et al. [6] were able to reduce thermal stresses and temperature gradients by decreasing the heating rate and the preheating temperature, which led to optimization of the net heat treatment duration.

The focus of this work is obtaining the temperature field of the components inside a heat treatment furnace. Thermal finite element analysis is implemented in commercial software to describe this non-linear and transient phenomenon. Several thermal scenarios are assessed by modifying the boundary conditions of the model to evaluate the response of the treated components to different heating/cooling rates and convection coefficients.

Francis turbine runners have geometries with high aspect ratio between external diameter and minimum wall thickness. For this reason, simplified models are necessary to reduce the computational cost while maintaining the quality of the finite element mesh. The numerical analysis is implemented following two approaches: first, the Francis turbine runner is subjected to boundary conditions directly applied on its external surfaces; second, both runner and furnace are included in the same model and heat transfer by convection and radiation is considered. Thus, the final results allow evaluating temperature gradients within the runner and the power input requirements to follow the heat treatment curve.

2 Methodology

2.1 Preprocessing

A CAD model of the Francis turbine runner considered in this work is shown in Figure 1 a). This 20-blade runner is made of COR 13-4 stainless steel, has an external diameter of 3.2m, height of 1.1m and weighs 16 metric tons. Cyclic symmetry is implemented for one blade of the runner to minimize computational cost. Mesh convergence was reached for the discretization of 223000 second order tetrahedral finite elements. Temporal convergence of the transient solution was guaranteed for a time step of 15 seconds.

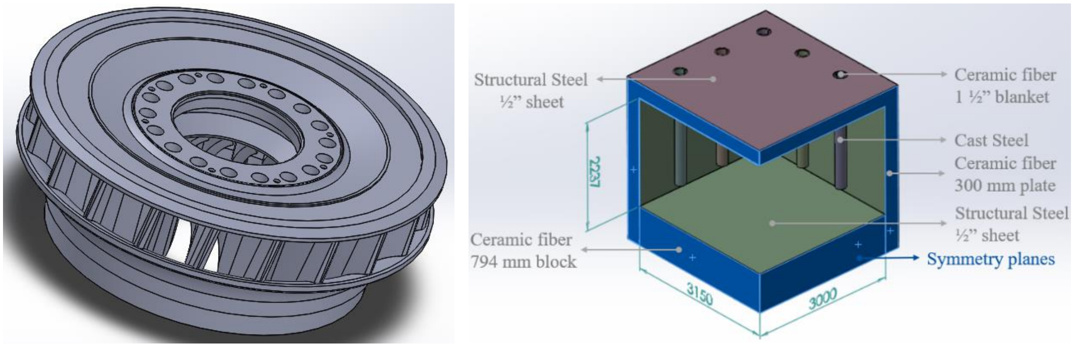

a) Francis turbine runner CAD b) Furnace dimensions and materials

Figure 1. Preproccessing data: Geometry, materials and symmetry

The heat treatment process of the runner is conducted in a box furnace (width 6.3m, length 6m and height 2.24m) with a sliding structure in the bottom to support the weight of the runner. The heating source corresponds to 20 radiant tubes of 202mm diameter. The walls of the furnace are multilayer, with ceramic fiber in the inner surface for insulation and steel in the external surface to provide structural support. The thickness of each layer and other relevant dimensions are shown in Figure 1 b). Only a quarter of the furnace is modelled to reduce computational cost and symmetry is considered in two planes through the center of the furnace. Mesh convergence is guaranteed for 118000 second order tetrahedral finite elements.

2.2 Boundary conditions

The model created only for the periodic runner sector consists of a component being heated in the external surface without considering the specific details of the power source. A temperature boundary condition changing with time is imposed to follow the heat treatment curve. In addition, convection is applied in some surfaces of the runner to simulate heat transfer from a fluid inside the furnace to contribute to temperature homogenization on the faces of the runner that do not receive direct radiation from the heating tubes. The aforementioned boundary conditions are represented in Figure 2. The transient phenomenon of this model is captured by changing the heating/cooling rate of the runner. Three values are considered for this parameter according to empirical knowledge of the process (see Table 1). The different configurations of the convection coefficient correspond to the values expected for furnaces with forced internal flow [9].

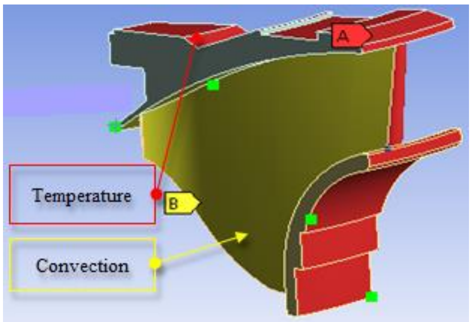

Figure 2. Boundary conditions on cyclic sector of the runner

The boundary conditions of the model including the furnace and the runner simultaneously are shown in Figure 3. Ambient convection and radiation are imposed for the external faces of the furnace. The inner walls of the furnace are subjected to heat exchange by convection with a fluid (not explicitly modelled) at 750°C. Surface to surface radiation (with perfect enclosure) is assumed among the radiant tubes of the furnace, its walls and the external faces of the runner. In this case, the heat source of the model is associated to a constant temperature of 1250°C on the radiant tubes. The parameters of the boundary conditions are shown in the Table 1

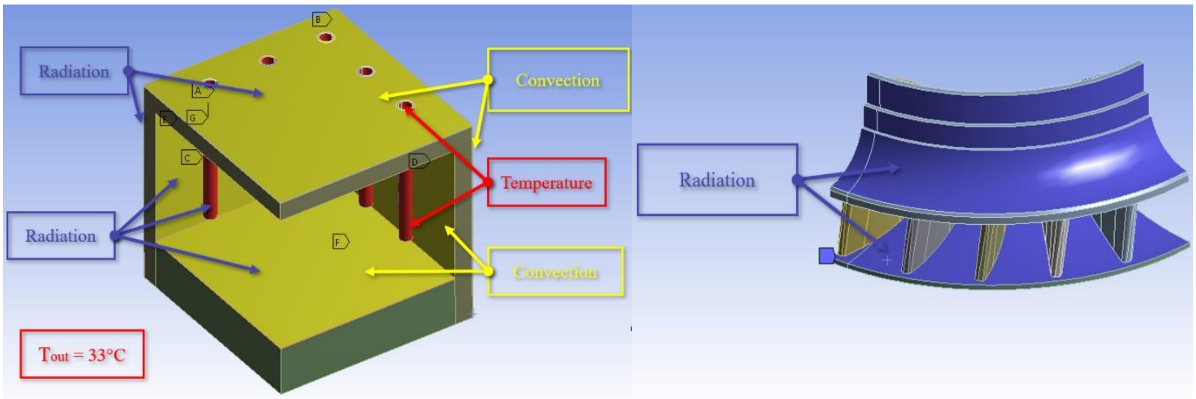

a) Furnace boundary conditions

b) Runner boundary conditions

Figure 3. Boundary conditions for the furnace and runner analysis

Table 1. Boundary conditions parameterers for each model

Case 1: Cyclic sector of the runner		**Case 2: Furnace and runner**	
Variable	**Value**	**Variable**	**Value**
Heating/Cooling rate (°C/h)	80	Inside convection fator (W/m² K)	3
	60	Outside convection fator (W/m² K)	25
	40	Runner emisivity	0.82
Convection coefficient (W/m² K)	150	Ceramic fiber emisivity	0.7
	175	Steel emisivity	0.82
	200	Outside temperture (°C)	33

3 Results

In the case of the model only with the runner, a lineal heating is considered, starting form ambient temperature and for the different combinations of the boundary conditions presented in Figure 2. The configuration with the highest heating rate (100°C/h) and the lowest convection coefficient (150W/m^{2}K) generates the highest temperature gradients within the runner. For this reason, this result is used as a reference to identify the regions where the measurement of temperature differences is critical to avoid any kind of damage on the runner. Figure 4 a), Figure 5 a) and Figure 6 a) show the maximum temperature difference over the selected critical path during the heating, for each heating rate and showing the dependence on the convection coefficient.

A similar analysis is implemented for the cooling stage. The initial temperature of the runner is assumed 620°C and is linearly cooled according to each cooling rate and configuration of convection coefficient. These results are shown in Figure 4 b), Figure 5 b) and Figure 6 b).

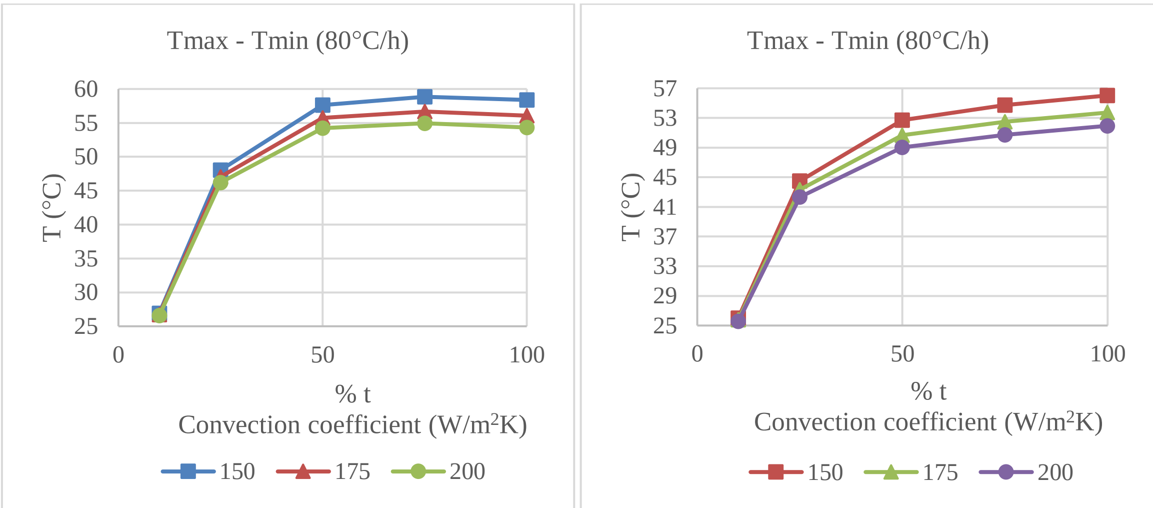

a) Heating at $80°C/h$

b) Cooling at $80°C/h$

Figure 4. Temperature difference in the critical region for a heating/cooling rate of 80°C/h

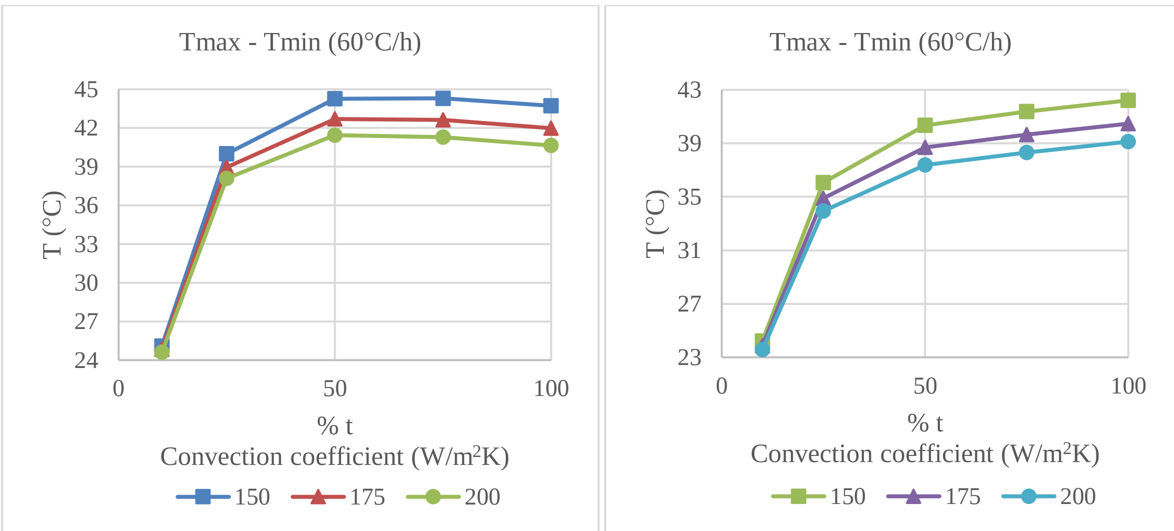

a) Heating at $60°C/h$

b) Cooling at $60°C/h$

Figure 5. Temperature difference in the critical region for a heating/cooling rate of 60°C/h

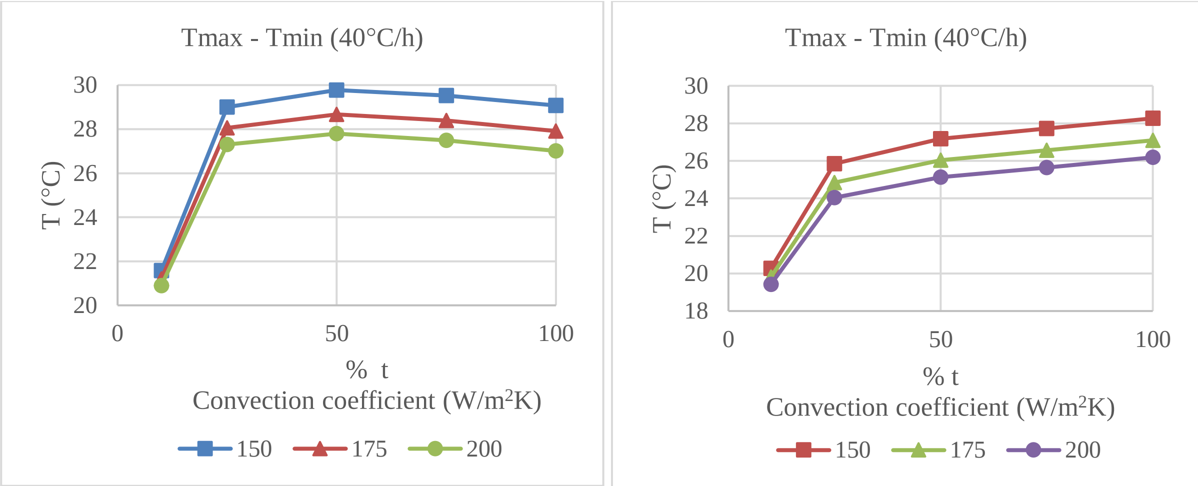

a) Heating at $40°C/h$ b) Cooling at $40°C/h$

Figure 6. Temperature difference in the critical region for a heating/cooling rate of 40°C/h

An empirical thermal criterion to avoid distortion and damage of components during heat treatment consists in keeping the maximum temperature gradient between surface and core below 50°C [3]. Thus, the previous results allow selecting the best scenario to satisfy this requirement while minimizing the duration of the entire heat treatment process. Figure 5 a) and Figure 5 b) show that damage can be avoided for the 60°C/h heating/cooling rate and the lowest convection coefficient (150W/m^{2}K), in which case the maximum temperature gradient is 44°C. Also, it is clear that the effect of convection on temperature homogenization of the runner is not significant, since the maximum temperature gradient can be decreased to 41°C if the convection coefficient corresponds to 200W/m^{2}K. Figure 4 a) and Figure 4 b) show that if higher heating/cooling rates are considered (for instance 80°C/h), values above 200W/m^{2}K need to be selected for the convection coefficient to keep the temperature gradient less than 50°C, which would require heat transfer by convection outside the common limits stated for box furnaces with radiant tubes.

The temperature field for the case of furnace and runner is shown in Figure 7 a) and the dependence of the input power with time is shown in Figure 7 b) for a quarter of the furnace. In this case, the boundary conditions selected for the model are such that the maximum heating power (4.8 MW) is required during the first seconds of the cycle due to the higher temperature gradients among the radiant tubes, the runner and the furnace walls.

4 Conclusions

The methodology implemented in this work allowed obtaining a numerical model to identify different thermal scenarios in which a Francis turbine runner can be heat treated with a control on the maximum temperature gradient to avoid damage induced by thermal stresses. Equivalent results were obtained for the heating and cooling stages of the heat treatment cycle. Thus, Figure 4, Figure 5 and Figure 6 showed that the effect of the convection coefficient on temperature homogenization is not significant (the maximum temperature difference is 5°C, which is a low value compared with the technological and power requirements to generate this level of forced convection.

On the other hand, the best thermal configuration from the perspective of temperature homogenization corresponds to the lowest heating/cooling rate and the highest convection coefficient. In this particular case study, the maximum temperature gradient can be kept significantly lower than 50°C for a heating/cooling rate of 40°C/h. However, the proposed heating/cooling rate for the analyzed runner is 60°C/h because it allows reducing the entire duration of the heat treatment process while satisfying the allowable limits of the temperature gradient. Finally, the model including the furnace and the runner simultaneously can be used as a first measurement of the maximum power that needs to be provided by each radiant tube and the total energy consumption of the heat treatment cycle. According to Figure 7, the most valuable results are those given on the first seconds of the heat treatment process because the maximum heat demand is required when the temperature gradients are higher. Nevertheless, energy consumption also depends on the heating rate, in such a way that the required power input is decreased for lower heating rates with the drawback of an increase on the total heat treatment duration.

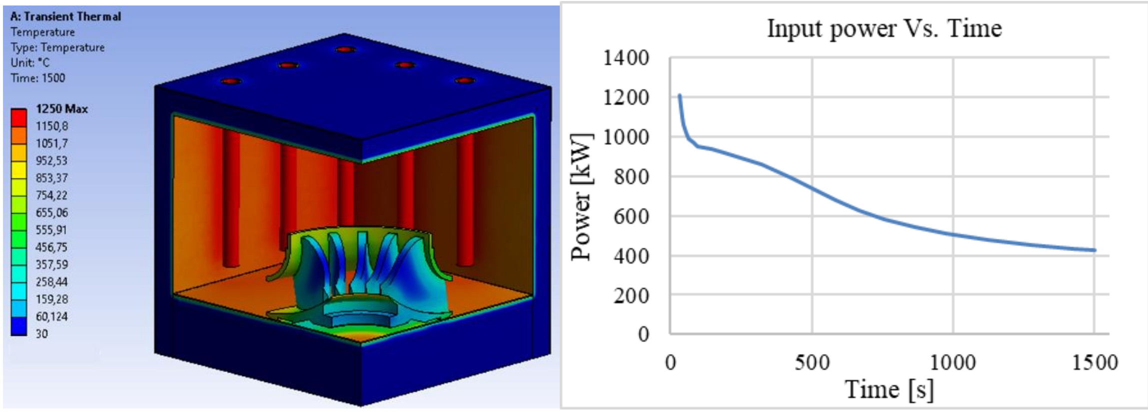

a) Furnace temperature field at 1500s b) Input power on radiant tubes

Figure 7. Results for the case including both furnace and runner

Acknowledgements. The authors are grateful for the support provided by the company EPM (Empresas Públicas de Medellín) with the project contract CW33433 (2018), the LDM (Laboratorio de Diseño Mecánico) and the DOA research group (Diseño y Optimización Aplicada).

Authorship statement. The authors hereby confirm that they are the sole liable persons responsible for the authorship of this work, and that all material that has been herein included as part of the present paper is either the property (and authorship) of the authors, or has the permission of the owners to be included here.

References

[1] I. Totten, *Steel heat treatment: Metallurgy and technologies*, Second. 2007.

[2] C. Şimşir and C. H. Gür, "A FEM based framework for simulation of thermal treatments: Application to steel quenching," *Comput. Mater. Sci.*, vol. 44, no. 2, pp. 588–600, 2008, doi: 10.1016/j.commatsci.2008.04.021.

[3] J. Li, J. Liu, Y. Tian, H. Wang, Y. Li, and Z. Wang, "Experimental and numerical study on optimization of heating process for small-sized workpieces in vacuum heat treatment furnace," *Heat Mass Transf. und Stoffuebertragung*, vol. 55, no. 5, pp. 1419–1426, 2018, doi: 10.1007/s00231-018-2512-2.

[4] X. Hao, J. Gu, N. Chen, W. Zhang, and X. Zuo, "3-D Numerical analysis on heating process of loads within vacuum heat treatment furnace," *Appl. Therm. Eng.*, vol. 28, no. 14–15, pp. 1925–1931, 2008, doi: 10.1016/j.applthermaleng.2007.12.007.

[5] X. Wan, Z. Dong, S. Li, and S. Liu, "Research on thermal stress of slab heating process based on transient non-linear analysis," *Adv. Mater. Res.*, vol. 311–313, pp. 936–939, 2011, doi: 10.4028/www.scientific.net/AMR.311-313.936.

[6] D. Ramanenka, G. Gustafsson, and P. Jonsén, "Influence of heating and cooling rate on the stress state of the brick lining in a rotary kiln using finite element simulations," *Eng. Fail. Anal.*, vol. 105, no. June, pp. 98–109, 2019, doi: 10.1016/j.engfailanal.2019.06.031.

[7] M. F. Santos *et al.*, "Enhanced numerical tool to evaluate steel ladle thermal losses," *Ceram. Int.*, vol. 44, no. 11, pp. 12831–12840, 2018, doi: 10.1016/j.ceramint.2018.04.092.

[8] A. Hou, S. Jin, H. Harmuth, and D. Gruber, "Thermal and Thermomechanical Responses Prediction of a Steel Ladle Using a Back-Propagation Artificial Neural Network Combining Multiple Orthogonal Arrays," *Steel Res. Int.*, vol. 90, no. 7, pp. 1–8, 2019, doi: 10.1002/srin.201900116.

[9] M. Gao, C. N. Reid, M. Jahedi, and Y. Li, "Estimating equilibration times and heating/cooling rates in heat treatment of workpieces with arbitrary geometry," *J. Mater. Eng. Perform.*, vol. 9, no. 1, pp. 62–71, 2000, doi: 10.1361/105994900770346295.